Predicting Intrinsic Clearance for Drugs and Drug Candidates Metabolized by Aldehyde Oxidase

ARTICLE *in* MOLECULAR PHARMACEUTICS · JANUARY 2013

Impact Factor: 4.38 · DOI: 10.1021/mp300568r · Source: PubMed

2 AUTHORS, INCLUDING:

Jeffrey P Jones
Washington State University
111 PUBLICATIONS **3,355** CITATIONS

molecular pharmaceutics

Article

pubs.acs.org/molecularpharmaceutics

Predicting Intrinsic Clearance for Drugs and Drug Candidates Metabolized by Aldehyde Oxidase

Jeffrey P. Jones* and Kenneth R. Korzekwa

Department of Chemistry, Washington State University, Pullman, Washington 99163, United States

Department of Pharmaceutical Sciences, Temple University School of Pharmacy, Philadelphia, Pennsylvania 19140, United States

Supporting Information

ABSTRACT: Metabolism by aldehyde oxidase (AO) has been responsible for a number of drug failures in clinical trials. The main reason is the clearance values for drugs metabolized by AO are underestimated by allometric scaling from preclinical species. Furthermore, in vitro human data also underestimates clearance. We have developed the first in silico models to predict both in vitro and in vivo human intrinsic clearance for 8 drugs with just two chemical descriptors. These models explain a large amount of the variance in the data using two computational estimates of the electronic and steric features of the reaction. The in vivo computational models for human metabolism are better than in vitro preclinical animal testing at predicting human intrinsic clearance. Thus, it appears that AO is amenable to computational prediction of rates, which may be used to guide drug discovery, and predict pharmacokinetics for clinical trials.

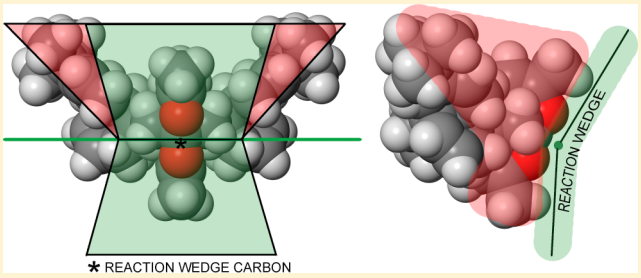

KEYWORDS: *drug metabolism, pharmacokinetics, aldehyde oxidase, AOX1, clearance*

Aldehyde oxidase (AO, EC1.2.3.1) is a cytosolic molybdoflavoenzyme present in many animal species, including humans. AO is a member of the xanthine oxidase family, which consists of complex metalloflavoproteins containing two [2Fe2S] clusters, FAD and the molybdenum cofactor (Moco) that are essential for enzyme activity.[1] As the name implies, AO can oxidize aldehydes to carboxylic acids, but the most important metabolic transformation is the oxidation of nitrogen containing aromatic compounds. We, and others, have described the mechanism of oxidation of azaheterocycles, which in most cases involves nucleophilic attack on an aromatic carbon adjacent to nitrogen[2,3] although it can also oxidize the carbon para to the nitrogen in some cases. For a detailed description of the possible mechanisms see Alfaro and Jones.[2] Since the drug pipeline has increasing numbers of azaheterocyclic compounds, in some cases AO will play an ever-increasing role in drug metabolism.[4,5] The major recognized problem with AO metabolism is the lack of reliable and predictive animal models using the normal preclinical animals, although it has been suggested that monkeys and guinea pigs may be reasonable models for humans.[5] Furthermore, variability in human AO activity in cytosol has also been documented[6,7] and in vitro predictions of in vivo metabolism using human cytosol underestimate clearance.[8,9]

While species differences have been known for some time,[10] three compounds have failed in clinical trials recently as a result of extensive AO metabolism.[11−13] Failures in clinical trials or late in the discovery process have economic implications. However the major impact is the loss of new therapeutic agents for debilitating or life-threatening diseases. A novel treatment for Parkinson's disease, FK3453, recently failed in phase I trials. Its predicted human intrinsic clearance was 1.3 mL/min/kg, while the actual intrinsic clearance in human can be roughly estimated from the data to be 3,000 mL/min/kg.[13] A selective c-MET inhibitor, SGX523, entered clinical trials as a promising treatment for solid tumors and failed as a result of AO metabolism that resulted in renal failure from crystal deposits in renal tubules.[12] Again, the failure is directly related to the lack of good models for human AO metabolism, but is related more to poor solubility of the metabolite than high clearance. Finally, a novel p38 MAP kinase inhibitor 6-(2,4-difluorophenoxy)-2-((*R*)-2-hydroxy-1-methyl-ethylamino)-8-((*S*)-2-hydroxypropyl)-8*H*-pyrido[2,3-*d*]pyrimidin-7-one developed for treatment of rheumatoid arthritis entered phase I trials with favorable predicted clearance.[11] The observed clearance was almost 10 times the predicted clearance based on allometric scaling leading to discontinuation of the clinical trials.

Despite the wide variation in potential substrate structures (Figure 1), examples of drugs for which AO is the primary enzyme involved in clearance are few. Zaleplon, a sedative drug used primarily for the treatment of insomnia, is a non-benzodiazepine hypnotic that is cleared primarily by AO.[14]

Special Issue: Predictive DMPK: In Silico ADME Predictions in Drug Discovery

Received: October 4, 2012
Revised: January 15, 2013
Accepted: January 30, 2013

dx.doi.org/10.1021/mp300568r | *Mol. Pharmaceutics* XXXX, XXX, XXX−XXX

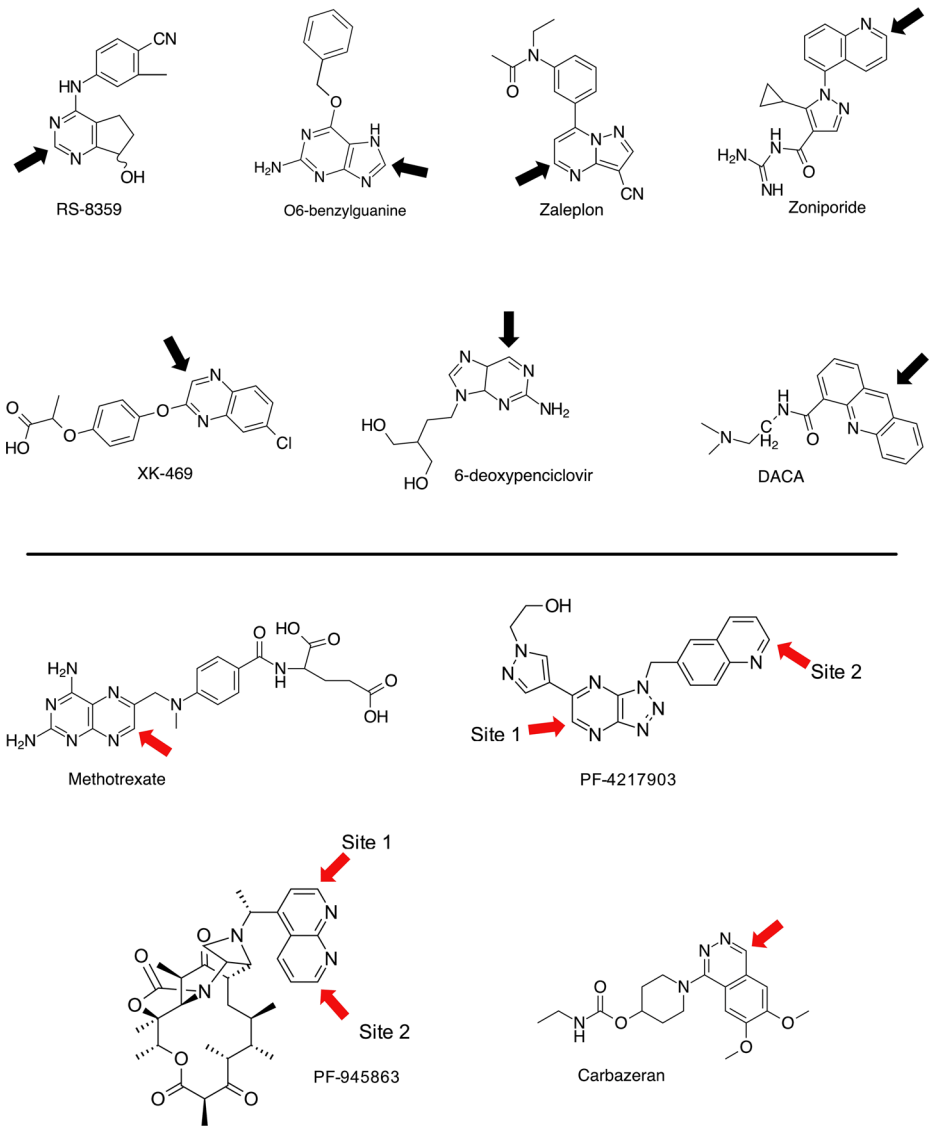

Figure 1. Compounds used to develop predictive models. Compounds used for intrinsic clearance predictions (training set) have black arrows pointing to the sites of oxidation. Compounds not used in the training set have red arrows pointing to the sites of oxidation.

Also, famciclovir, an antiviral prodrug used primarily to treat herpes virus infections, is activated by AO to its active 6-oxo form, penciclovir.[15] Ziprasidone, which is used to treat the symptoms of schizophrenia,[16] is metabolized by AO, as are the anticancer agents methotrexate[17] and zebularine.[18] AO is also involved, or has been implicated, in the secondary metabolism of other drug metabolites.[19]

Based on the analysis of Pyrde et al., it is expected that AO will play an increasing role in drug metabolism.[4] Computational models will be important in drug design and in determining potential clearance of compounds in clinical trials. To date only two studies have reported any modeling efforts: The first was a homology model and docking study on a series of nondrug molecules.[20] The second study predicted the regioselectivity of AO metabolism for both nondrug and drug candidates using density functional theory (DFT) quantum chemical methods.[21] This model is the basis for the rate-prediction models reported herein. Predicted in vivo and in vitro clearance values are found to be close to reported values. Since this model is mechanistic, the methodology can be applied to compounds not related to the training set.

RESULTS

Compounds and Sites of Oxidation. We used 7 of the compounds shown in Figure 1 to assess our ability to use the electronic and steric features of drugs to model their intrinsic hepatic clearance. These compounds were used by Zientek and co-workers[9] to test for in vitro−in vivo correlations. The other compounds shown in Figure 1 were not used in modeling intrinsic clearance for various reasons. Carbazeran has recently been reported to be cleared mainly by formation of a glucuronide conjugate.[22] Methotrexate is primarily cleared by renal secretion, is not cell permeable, and requires transporters to enter and leave the hepatocyte (Swati Nagar and Vaishnavi Ganti, personal communication). Since the intracellular hepatic concentration of methotrexate is unknown, it would be difficult to compare in vitro and in vivo intrinsic clearances. However, methotrexate is an excellent substrate for determining unfavorable steric interactions since it has very favorable chemical reactivity, but the site of metabolism is very hindered (Table 1).

The two Pfizer compounds in Figure 1 (PF-945863 and PF-4217903) have not had the site of metabolism reported in the

dx.doi.org/10.1021/mp300568r | Mol. Pharmaceutics XXXX, XXX, XXX−XXX

Table 1. Relative Heats of Reaction, Steric Hindrance, in Vivo and in Vitro Intrinsic Clearance Values and Predicted Values

compound	Hr_{Rel}[a]	steric[b]	$CL'_{int,AO,H}$ in vivo[c]	pred $CL'_{int,AO,H}$ in vivo[d]	$CL'_{int,AO,HP}$ in vivo[c]	pred $CL'_{int,AO,HP}$ in vivo[d]	$CL'_{int,AO,H}$ in vitro[e]	pred CL in vitro[f]
RS-8359	4.41	8.3	23	27.2	14.3	17	7.1	11.3
6-deoxypenciclovir	2.78	8.6	140	45.9	94	26	29	14.5
zoniporide	−0.22	3.8	180	230.9	51.3	90	37	42.2
zaleplon	−1.07	8	65	185.4	29.7	81	6.1	30.3[g]
XK469	−2.66	32	16	17.2	16	18	2.5	2.6
O6-benzylguanine	−3.53	9.2	360	373.2	157	148	36	40.5
DACA	−8.48	8.3	3600	2283.5	1080	651	111	105.9
PF-4217903[g]	2.84	13	46	26.3	32	18	2.2[h]	8.71[h]
PF-945863[g]	−4.19	9.35	180	459.8	148	177	35[i]	44.6[i]
PF-4217903[g]	2.91	9.43	46	39.6	32	23	2.2[i]	12.9[i]
PF-945863[g]	−3.28	9.18	180	343.3	148	138	35[h]	38.8[h]
carbazaran[g]	−0.61	8.7	13000	145.3	ND[j]	ND[j]	323	25.8
methotrexate[g]	−8.38	17	0.44	764.7	ND[j]	ND[j]	2.5	38.5

[a]The heat of reaction relative to quinoline as described in Results in kcal/mol. [b]The steric effect predicted by interaction with wb17 in kcal/mol. [c]In vivo hepatic intrinsic clearance as reported in ref 9 in mL/min/kg. [d]The predicted hepatic clearance value from eq 2 in mL/min/kg. [e]In vitro intrinsic clearance as reported in ref 9 in mL/min/kg. [f]The predicted clearance value from eq 3 when the hepatic clearance is corrected for 30% pulmonary clearance. [g]Red color indicates these points of compounds were not used in the correlations to produce eq 2 and eq 3. [h]This is the clearance prediction for site 1 of the corresponding compound as in Figure 1 in mL/min/kg. [i]This is the clearance prediction for site 2 of the corresponding compound as shown in Figure 1 in mL/min/kg. [j]Not determined.

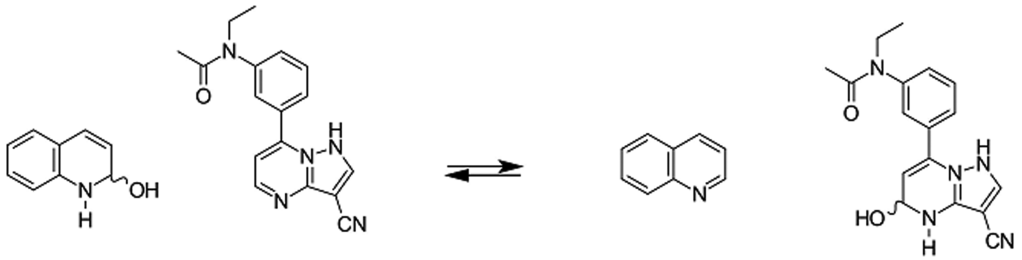

Figure 2. An example of the determination of the relative heat of reaction, Hr_{Rel}. Hr_{Rel} is the difference in energy for water addition to quinoline and water addition to the AO substrate. In this case the zaleplon water addition product is exothermic (−1.07 kcal/mol).

literature to our knowledge. Also, PF-945863 is a very large molecule that is difficult to treat with the DFT calculations so an abbreviated version was used to determine the electronic and steric propensity for reaction. The two Pfizer compounds serve as an external validation set. In each case two metabolites are possible and we used the stability of the tetrahedral intermediate to determine the most favored site, which was then used to predict in vivo or in vitro clearance based on the appropriate equation shown below. The electronic and steric values for all compounds were determined and are given in Table 1. In addition to the intrinsic clearance values calculated by Zientek et al., we also considered the possibility of metabolism by extrahepatic AO. An additional set of in vivo unbound intrinsic clearances were calculated based on an assumption that 30% of the AO activity is due to extrahepatic metabolism. Although the extent and location of extrahepatic AO metabolism is unknown, these values provide an indication of the impact that extrahepatic AO will have on in vivo intrinsic clearances.

Prediction of the Electronic Propensity for Reaction. The potential for reaction at a given site is dependent on the ability of the molecule to accept the equivalent of a hydroxide at the site of oxidation, and rates are related to the stability of the tetrahedral intermediate formed during the reaction.[2,3] Previously we used the heat of reaction of the tetrahedral intermediate to predict the site of metabolism for a number of compounds.[21] To determine the electronic favorability of a given reaction we calculated the difference in energy between the drug and the tetrahedral intermediate after addition of water to the parent drug. The values relative to quinolone are given as Hr_{Rel} in Table 1 (see Figure 2 and Methods). Compounds with a more stable tetrahedral intermediate relative to quinoline have negative relative heats of reaction, while less stable intermediates have positive relative heats of reaction. Multiple products were explored for the Pfizer compounds. For PF-945863 site 2 has the lowest energy tetrahedral intermediate by 0.91 kcal/mol, and for PF-4217903 site 1 has the lowest energy tetrahedral intermediate by 0.07 kcal/mol (Figure 1). This suggests that both products are formed in similar amounts for both compounds.

Prediction of the Steric Propensity for Reaction. For AO to mediate the nucleophilic addition of water to an aromatic system it must have access to the Π* antibonding orbital of the aromatic system. Given the structure of Moco, the site of oxidation must fit in a reactivity wedge between the equatorial sulfur and hydroxide equivalent. Figure 3 shows the transition state for the oxidation of quinazolinone reacting with an abbreviated Moco.

Furthermore, the protein around the cofactor should modulate access to the wedge in the transition state. Since the structure of human AO has not been solved, we developed a steric probe to simulate the steric constraints associated with the protein. The steric probe (WB17) is shown in Figure 4 with the low steric reaction wedge in green and the sterically

dx.doi.org/10.1021/mp300568r | Mol. Pharmaceutics XXXX, XXX, XXX−XXX

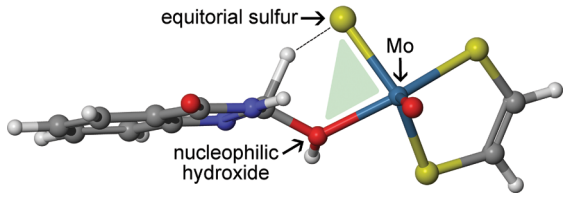

Figure 3. The transition state for the oxidation of 4-quinazolinone by a Moco model. The equatorial sulfur and the nucleophilic hydroxide form the reaction wedge shown in green.

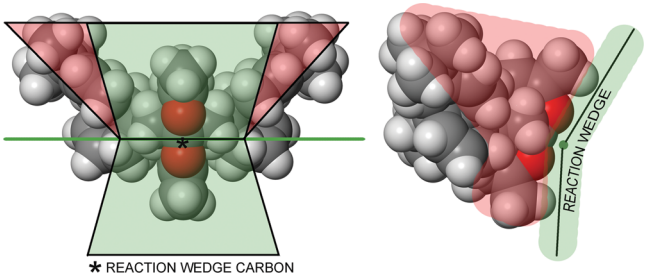

Figure 4. Description of steric surrogate for AO protein. The reaction wedge carbon is used to tether the reactive carbon's hydrogen atom and the substrate pulled into the reaction wedge to simulate the steric effect associated with the active site.

hindered sites in red. The Cartesian coordinates are provided in the Supporting Information. The complex nature of this steric probe ensures low conformational mobility and a plane of symmetry. This steric probe was designed based on the ability of DACA with three fused rings to approach with limited steric hindrance, and the molecule's ability to block approach of methotrexate and XK-469, which are both electronically favorable but have very low levels of AO metabolism. In short the probe needed to have low steric hindrance in the "reaction wedge" and higher steric hindrance above and below the wedge. Energies were determined as described in Methods.

Prediction of Intrinsic Hepatic Clearance. Intrinsic clearance was correlated with the combined steric and electronic properties using eq 1:

$$\ln(\text{pred } CL'_{\text{int,AO}}) = A\ \text{Hr}_{\text{Rel}} + B\ \text{steric} + C \quad (1)$$

The fits to the in vivo results based on hepatic AO only provided the following model:

$$\ln(\text{pred } CL'_{\text{int,AO,H}}) = -0.174\ \text{Hr}_{\text{Rel}} - 0.114\ \text{steric} + 4.14,\ r^2 = 0.92,\ n = 7 \quad (2)$$

The fits to the in vivo results based on 70% hepatic AO and 30% extrahepatic AO provided the following model:

$$\ln(\text{pred } CL'_{\text{int,AO,HP}}) = -0.285\ \text{Hr}_{\text{Rel}} - 0.081\ \text{steric} + 4.74,\ r^2 = 0.76,\ n = 7 \quad (3)$$

The fits to the in vitro results provided the following model:

$$\ln(\text{pred } CL'_{\text{int,AO,H}}) = -0.344\ \text{Hr}_{\text{Rel}} - 0.212\ \text{steric} + 5.83,\ r^2 = 0.87,\ n = 6 \quad (4)$$

The predicted intrinsic clearance values are given in Table 1. The agreement between the fitted and the actual values is given in Figure 5a–c. For the in vitro correlation, zaleplon was excluded as an outlier, but the predicted value is included in Figure 5c.

DISCUSSION

As a result of an increase in nitrogen containing aromatic rings in new drug candidates, AO is an increasingly important drug

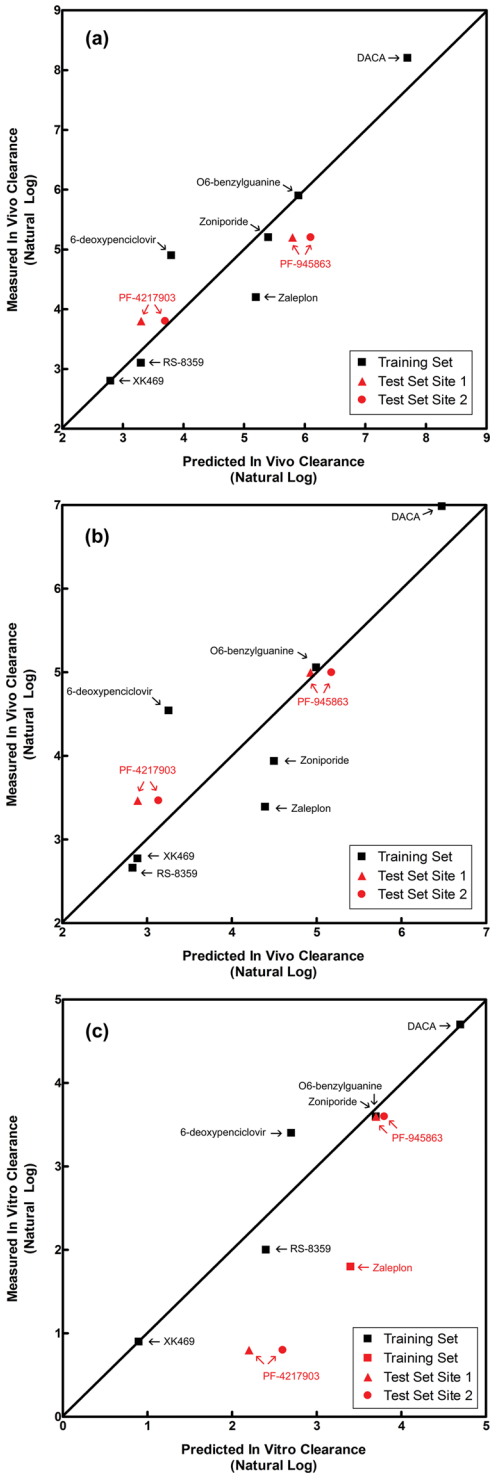

Figure 5. (a) In vivo versus predicted in vivo clearance based on hepatic AO alone. (b) In vivo versus predicted in vivo clearance based on 70% hepatic and 30% pulmonary AO. (c) In vitro versus predicted in vitro intrinsic clearance. All values have the units mL/min/kg.

dx.doi.org/10.1021/mp300568r | Mol. Pharmaceutics XXXX, XXX, XXX–XXX

metabolizing enzyme.[5] Nitrogen has been introduced for both pharmacokinetic and pharmacodynamic reasons.[23,24] With some exceptions, nitrogen decreases the clearance associated with cytochrome P450 enzymes,[25,26] leading to better pharmacokinetics that results from a longer half-life. More recently, the kinase family of enzymes have become drug targets for a number of diseases and the pharmacophore for these enzymes almost always includes a nitrogen. The unexpected consequence of this increase in azoheterocycles has been an increase in drug failures in clinical trials as a result of unexpected high AO clearance.[4]

Preclinical animal models in general fail to predict human AO mediated metabolism.[5] Rodent AO shows different rates and selectivities relative to the human enzyme. Dogs appear to have no active AO. Thus, both rodents and dogs underpredict clearance.

In vitro screens with human AO have also proven misleading for three reasons: (1) Many in vitro screens only use microsomal cell fractions, while AO is a cytosolic enzyme. (2) AO appears to be relatively unstable, leading to variability in different cytosolic preparations. (3) A large fraction of the drugs metabolized by AO have very high extraction ratios with predicted intrinsic clearance values higher than liver blood flow.[8] In fact a number of the compounds in Table 1 have intrinsic clearance values higher than the liver blood flow (20.7 mL/min/kg). At present it is not known what tissue besides the liver is responsible for the high rate of metabolism making in vitro−in vivo scaling difficult. The net result is that in vitro data has only proven to be able to give rank order correlation with in vivo metabolic rates.[9]

In order to fill the need for preclinical estimations of clearance we developed a computational model that predicts human intrinsic clearance. The model is scaled to human in vivo data, and thus "corrects for" the high clearance compounds such as DACA which has an in vivo human intrinsic clearance of 3.6 L/min/kg. This model is mechanistic and contains two parameters: (1) the electronic propensity for reaction estimated by the ground state energies of the substrate and tetrahedral intermediate and (2) a term estimating the steric component of the transition state.

Each of the oxidation sites is shown in Figure 1. The black arrows indicate compounds and sites used to develop the predictive models given in eq 2 and eq 3. For the in vitro model (eq 3) zaleplon was left out of the fit and its clearance predicted. (Note: Zaleplon in vitro measurements have proved problematic for other researchers.[8] It is not clear if the error is in the computational method or the in vitro data.) Overall, the fits are very good for both the in vivo and in vitro data (Figure 5). To our knowledge this is the largest group of in vivo clearance values correlated with mechanistic descriptors to produce an intrinsic prediction model.

Still, the data set is limited and assumptions are required to calculate in vivo hepatic intrinsic clearances. One assumption is that clearance by AO occurs exclusively in the liver. In order to determine the impact that extrahepatic metabolism would have on calculated in vivo intrinsic clearances, we generated a set of $CL'_{int,AO}$ values based on 30% pulmonary metabolism. (Note: The 30% value was chosen arbitrarily to illustrate the effect of extrahepatic metabolism.) Also, only CL/F (F = bioavailability) can be determined with oral data alone, and calculating intrinsic clearances requires calculating F. Since $F = F_a \times F_g \times F_h$ (F_a, F_g, and F_h are the fractions absorbed, escaping gut metabolism, and escaping hepatic metabolism, respectively), F can only be calculated if F_a and F_g are assumed to be 1. The equations used to calculate $CL'_{int,AO,HP}$ values are given in Methods, and the values are given in Table 1.

For the compounds with oral data only (RS-8359, 6-deoxypenciclovir, PF-42179037, and PF-9458637), the calculated $CL'_{int,AO}$ values will be lower if F_a and/or F_g are less than 1. The antiviral 6-deoxypenciclovir has a reported $CL'_{int,AO,H}$ of 140 mL/min/kg and a calculated $CL'_{int,AO,HP}$ of 94 mL/min/kg based on the assumptions that the famciclovir is completely converted to 6-deoxypenciclovir and that 6-deoxypenciclovir is not subject to intestinal metabolism. The $CL'_{int,AO}$ value will be lower if these assumptions are not valid.

Therefore, there is significant uncertainty associated with many of the $CL'_{int,AO}$ values. However, when an assumption of extrahepatic metabolism is included, most of the data remains in the same order of intrinsic clearance and the fits to the in vivo data are similar. Due to the small size of the data set, incorrect assumptions can result in significant differences in the fits. For example, for the hepatic/pulmonary model, removal of 6-deoxypenciclovir from the training set changes the r^2 value from 0.76 to 0.93. Obviously, additional data is needed for more accurate parametrization of an in vivo model.

To assess the models' ability to predict the clearance of compounds not in the training set we used two Pfizer compounds whose intrinsic clearance was reported without the site of oxidation. Both of these compounds are reported by Zientek and co-workers[9] to be exclusively cleared by AO. The red arrows indicate potential sites of oxidation for PF-4217903 and PF-945863. Two methods can be used to predict which site will be the site of metabolism. The first method is to use the stability of the tetrahedral intermediate. For PF-4217903 site 1 was predicted to be the major site of metabolism; however, the difference in the tetrahedral intermediates is a trivial 0.07 kcal/mol. For PF-945863 the difference between the energy of the two sites is also very small with a slight preference for site 2. The second method is to look at the predicted clearance values for each pathway. This method favors site 2 for PF-4217903 and PF-945863. It is worth noting that either site gives similar predicted clearance rates, and that both are close to the actual clearance values. While the fit of PF-4217903 appears to deviate from the line of ideal agreement for the in vitro plots (Figure 5c), the actual clearance value is 2.2 mL/min/kg while the predicted values range from 8.7 to 12.9 mL/min/kg. This is not a large error relative to the range of all the data (2.5−111 mL/min/kg). The predicted values for PF-945863 in vitro range from 38.8 to 44.6 mL/min/kg compared with the actual value of 35 mL/min/kg and is in very close agreement. Surprisingly, the in vivo correlations are close to those for the in vitro correlations. This could be a result of variance in the in vitro data as a result of enzyme instability, or it could result from differences in in vitro versus in vivo substrate inhibition. Differences in substrate inhibition have been observed in vitro, with our group seeing no substrate inhibition with phthalazine,[27] while Obach reported significant substrate inhibition.[28] Finally, it could just be a result of having a relatively small data set. Overall, it is clear that eq 2 can predict in vivo clearance of the test set better than the in vitro experimental.

From looking at the structures of the substrates in Figure 1, one can make certain deductions about the structure of the active site. First, since the structures are diverse, the enzyme most likely is very flexible, or has a very open active site. This is consistent with complex inhibition kinetics, which requires

multiple binding sites.[26] Second, the ability to bind molecules like PF-945863 indicates that parts of the substrate are likely to remain in the solvent during metabolism. Third, steric constraints are mostly associated with the area on the molecule close to the site of oxidation. Overall, the conclusion is that AO can metabolize large molecules, but that steric bulk outside the plane of the reaction wedge made by the Moco reaction center can slow metabolism.

CONCLUSIONS

While AO plays a minor role in drug metabolism, it has played a larger role in drug failures in clinical trials. This is a result of poor allometric scaling from preclinical species combined with in vitro screening that focuses on microsomal metabolism. Increased awareness has led many pharmaceutical companies to increase screening with cytosol to help determine if AO may play a role in metabolism. However, in vitro/in vivo scaling has not been particularly effective and often underestimates clearance. This is further complicated by reports of variability in cytosolic AO activities. To this end we developed a mechanistic computational model to predict intrinsic clearance. This model performs better than in vitro metabolism studies at predicting in vivo intrinsic clearance for the compounds tested. One caveat is that this model does not predict if a molecule will be an AO substrate, only the compound's clearance if it is a substrate. In this regard in vitro screening would complement the model by establishing if a compound is an AO substrate. Furthermore, within the lead optimization process, it can be used presynthesis to remove AO liabilities and to estimate human clearance of possible drug candidates. Since the model is mechanistic, it can be applied to compounds outside the training set.

MATERIALS AND METHODS

DFT Calculations. Tetrahedral intermediate structures were generated by considering the geometry optimized, neutral substrate, unless otherwise noted, where the nucleophile, $-OH^-$, attacks a carbon atom. For nitrogen-containing heterocycles, a hydrogen atom was added to the nitrogen, resulting in a net addition of water, in accordance with the proposed mechanism. All geometries and energies reported in this study were computed using the B3LYP density functional theory method,[28] implemented in the Gaussian03 program package.[28] Structures were optimized using DFT B3LYP functional and the 6-31G** basis set (B3LYP/6-31G**). The zero point energies were determined by a frequency calculation on the B3LYP/6-31G** optimized geometries. The single point energies were determined with the B3LYP functional and the 6-311+G(2d,2p). The Cartesian coordinates of the optimized structures are given in the Supporting Information. Typical errors observed for the B3LYP functional are in the range of 2−3 kcal/mol in calculations of reaction barriers and for complexes that do not contain transition metals, which may vary depending on the reaction being examined. Hessians were determined at the B3LYP/6-31G(d,p) level. Complete thermochemical calculations were performed, and final energies reported include zero-point vibrational energies.

Molecular Mechanics Calculations. Coordinate scans were done with MacroModel 9.9 using the OPLS 2005 force field in water with a constant dielectric. All compounds were properly ionized for pH 7.4 using Schrodinger LigPrep. To perform a scan two angles and one dihedral were held constant with a 100 kcal/mol potential. The angles were from the carbon in the reaction wedge to the H−C of the reacting bond, and from the carbon directly behind the carbon in the reaction wedge to the carbon in the reaction wedge and finally the carbon to be oxidized. Both these angles were fixed at 180 degrees and ensured similar steric interaction for different shaped substrates. The dihedral O−C−C−N between the lower oxygen, the reaction cleft carbon, the oxidized carbon and the adjacent nitrogen was held constant at 90 degrees. This dihedral prevented twisting when steric interactions were unsymmetrical. During each step of the coordinate scan (every 0.2 Å) 5000 steps of minimization were performed. Relative steric energies were determined by varying the distance between the hydrogen on the carbon to be oxidized and the carbon between the oxygens shown in red on WB17 between 2.2 Å and 6 Å in 0.2 Å increments (an example energy curve for PF-4217903 is given in Figure s1 in the Supporting Information, while the approach of DACA to WB17 is shown in Figure s2 in the Supporting Information). The lowest energy was always between 2.8 and 3.2 Å, and the energy difference from the lowest energy and the energy at 2.4 Å was used to approximate steric hindrance to reaction. Rotation of the drug relative to WB17 was fixed with constraints as described in Methods. Scans were run in both directions to check for hysteresis. The difference in energy between 2.4 Å and the lowest energy is given in the steric column of Table 1.

Inclusion of Pulmonary AO When Calculating in Vivo $CL'_{int,AO}$. In order to evaluate the effect of extrahepatic AO, values of $CL'_{int,AO}$ were calculated with the assumption that 30% of the AO activity results from pulmonary AO. For iv administered drugs, the following equation was used to calculate hepatic $CL'_{int,AO}$:

$$CL_{obs} = \frac{Q_H(0.7)\frac{1}{f_{AO,H}} CL'_{int,AO} \frac{f_u}{BPR}}{Q_H + (0.7)\frac{1}{f_{AO,H}} CL'_{int,AO} \frac{f_u}{BPR}} + \frac{Q_P(0.3)\, CL'_{int,AO} \frac{f_u}{BPR}}{Q_P + (0.3)\, CL'_{int,AO} \frac{f_u}{BPR}} + CL_r \quad (5)$$

where CL_{obs} is the observed plasma clearance upon iv dosing, Q_H is liver blood flow (21 mL/min/kg), $f_{AO,H}$ is the fraction of liver elimination mediated by AO, BPR is the blood-to-plasma ratio f_u is the fraction unbound in plasma, Q_P is pulmonary blood flow (71 mL/min/kg), CL_r is the renal clearance, and $CL'_{int,AO}$ is the total intrinsic unbound clearance mediated by AO. For oral dosing, the additional assumptions that $F_a = 1$ and $F_g = 1$ must be made, where F_a is the fraction absorbed and F_g is the fraction that escapes gut metabolism. In the absence of renal clearance, eq 5 can be divided by 1 − ER (ER is the hepatic extraction ratio) to give eq 6:

$$CL_{obs} = \frac{\frac{Q_H(0.7)\frac{1}{f_{AO,H}} CL'_{int,AO} \frac{f_u}{BPR}}{Q_H + (0.7)\frac{1}{f_{AO,H}} CL'_{int,AO} \frac{f_u}{BPR}} + \frac{Q_P(0.3)\, CL'_{int,AO} \frac{f_u}{BPR}}{Q_P + (0.3)\, CL'_{int,AO} \frac{f_u}{BPR}}}{1 - \frac{(0.7)\frac{1}{f_{AO,H}} CL'_{int,AO} \frac{f_u}{BPR}}{Q_H + (0.7)\frac{1}{f_{AO,H}} CL'_{int,AO} \frac{f_u}{BPR}}} \quad (6)$$

Using these assumptions and equations $CL'_{int,AO}$ values can be calculated for the hypothetical situation of 70% liver AO and 30% pulmonary AO. Although the contribution of extrahepatic

dx.doi.org/10.1021/mp300568r | Mol. Pharmaceutics XXXX, XXX, XXX−XXX

AO is unknown, values and fits can be compared to the hepatic only models.

Regression analyses. MatLab 7.11 was used for the regression of the clearance values on the relative heat of reaction (Hr_{Rel}) and steric parameters.

■ ASSOCIATED CONTENT

Supporting Information

Figures describing the steric interaction model and Cartesian coordinates for all the calculated structures. This material is available free of charge via the Internet at http://pubs.acs.org.

■ AUTHOR INFORMATION

Corresponding Author

*Tel: 509-592-8790. E-mail: jpj@wsu.edu.

Notes

The authors declare no competing financial interest.

■ ACKNOWLEDGMENTS

The study was supported by a grant from the National Institute of General Medical Sciences, GM100874, and Pittsburgh Supercomputing Center Grant CHE100016P. We thank Swati Nagar for helpful comments and help with the extrahepatic modeling.

■ ABBREVIATIONS USED

AOX1, aldehyde oxidase 1; AO, aldehyde oxidase; Moco, molybdopterin cofactor; CL_{int}, intrinsic clearance; DFT, density functional theory

■ REFERENCES

(1) Schumann, S.; Terao, M.; Garattini, E.; Saggu, M.; Lendzian, F.; Hildebrandt, P.; Leimkuhler, S. Site directed mutagenesis of amino acid residues at the active site of mouse aldehyde oxidase AOX1. *PLoS One* **2009**, *4*, e5348.

(2) Alfaro, J. F.; Jones, J. P. Studies on the Mechanism of Aldehyde Oxidase and Xanthine Oxidase. *J. Org. Chem.* **2008**, *73*, 9469−9472.

(3) Okamoto, K.; Matsumoto, K.; Hille, R.; Eger, B. T.; Pai, E. F.; Nishino, T. The crystal structure of xanthine oxidoreductase during catalysis: Implications for reaction mechanism and enzyme inhibition. *Proc. Nat. Acad. Sci.U.S.A.* **2004**, *101*, 7931−7936.

(4) Pryde, D. C.; Dalvie, D.; Hu, Q.; Jones, P.; Obach, R. S.; Tran, T. D. Aldehyde oxidase: an enzyme of emerging importance in drug discovery. *J. Med. Chem.* **2010**, *53*, 8441−8460.

(5) Garattini, E.; Terao, M. Increasing recognition of the importance of aldehyde oxidase in drug development and discovery. *Drug Metab. Rev.* **2011**, *43*, 374−386.

(6) Al-Salmy, H. S. Individual variation in hepatic aldehyde oxidase activity. *IUBMB Life* **2001**, *51*, 249−253.

(7) Hartmann, T.; Terao, M.; Garattini, E.; Teutloff, C.; Alfaro, J. F.; Jones, J. P.; Leimkühler, S. The impact of single nucleotide polymorphisms on human aldehyde oxidase. *Drug Metab. Dispos.* **2012**, *40*, 856−864.

(8) Hutzler, J. M.; Yang, Y. S.; Albaugh, D.; Fullenwider, C. L.; Schmenk, J.; Fisher, M. B. Characterization of aldehyde oxidase enzyme activity in cryopreserved human hepatocytes. *Drug Metab. Dispos.* **2012**, *40*, 267−275.

(9) Zientek, M.; Jiang, Y.; Youdim, K.; Obach, R. S. In vitro-in vivo correlation for intrinsic clearance for drugs metabolized by human aldehyde oxidase. *Drug Metab. Dispos.* **2010**, *38*, 1322−1327.

(10) Garattini, E.; Mendel, R.; Romão, M. J.; Wright, R.; Terao, M. Mammalian molybdo-flavoenzymes, an expanding family of proteins: structure, genetics, regulation, function and pathophysiology. *Biochem. J.* **2003**, *372*, 15−32.

(11) Zhang, X.; Liu, H. H.; Weller, P.; Zheng, M.; Tao, W.; Wang, J.; Liao, G.; Monshouwer, M.; Peltz, G. In silico and in vitro pharmacogenetics: aldehyde oxidase rapidly metabolizes a p38 kinase inhibitor. *Pharmacogenomics J.* **2010**, *11*, 15−24.

(12) Diamond, S.; Boer, J.; Maduskuie, T.; Falahatpisheh, N.; Li, Y.; Yeleswaram, S. Species-Specific Metabolism of SGX523 by Aldehyde Oxidase and the Toxicological Implications. *Drug Metab. Dispos.* **2010**, *38*, 1277−1285.

(13) Akabane, T.; Tanaka, K.; Irie, M.; Terashita, S.; Teramura, T. Case report of extensive metabolism by aldehyde oxidase in humans: Pharmacokinetics and metabolite profile of FK3453 in rats, dogs, and humans. *Xenobiotica* **2011**, *41*, 372−384.

(14) Kawashima, K.; Hosoi, K.; Naruke, T.; Shiba, T.; Kitamura, M.; Watabe, T. Aldehyde oxidase-dependent marked species difference in hepatic metabolism of the sedative-hypnotic, zaleplon, between monkeys and rats. *Drug Metab. Dispos.* **1999**, *27*, 422−428.

(15) Filer, C. W.; Ramji, J. V.; Allen, G. D.; Brown, T. A.; Fowles, S. E.; Hollis, F. J.; Mort, E. E. Metabolic and pharmacokinetic studies following oral administration of famciclovir to the rat and dog. *Xenobiotica* **1995**, *25*, 477−490.

(16) Beedham, C.; Miceli, J. J.; Obach, R. S. Ziprasidone metabolism, aldehyde oxidase, and clinical implications. *J. Clin. Psychopharmacol.* **2003**, *23*, 229−232.

(17) Jordan, C. G.; Rashidi, M. R.; Laljee, H.; Clarke, S. E.; Brown, J. E.; Beedham, C. Aldehyde oxidase-catalysed oxidation of methotrexate in the liver of guinea-pig, rabbit and man. *J. Pharm. Pharmacol.* **1999**, *51*, 411−418.

(18) Klecker, R. W.; Cysyk, R. L.; Collins, J. M. Zebularine metabolism by aldehyde oxidase in hepatic cytosol from humans, monkeys, dogs, rats, and mice: influence of sex and inhibitors. *Bioorg. Med. Chem.* **2006**, *14*, 62−66.

(19) Kitamura, S.; Sugihara, K.; Ohta, S. Drug-metabolizing ability of molybdenum hydroxylases. *Drug Metab. Pharmacokinet.* **2006**, *21*, 83−98.

(20) Dastmalchi, S.; Hamzeh-Mivehrod, M. Molecular Modelling of Human Aldehyde Oxidase and Identification of the Key Interactions in the Enzyme-Substrate Complex. *Daru, J. Pharm. Sci.* **2005**, *13*.

(21) Torres, R. A.; Korzekwa, K. R.; McMasters, D. R.; Fandozzi, C. M.; Jones, J. P. Use of density functional calculations to predict the regioselectivity of drugs and molecules metabolized by aldehyde oxidase. *J. Med. Chem.* **2007**, *50*, 4642−4647.

(22) Sharma, R.; Strelevitz, T. J.; Gao, H.; Clark, A. J.; Schildknegt, K.; Obach, R. S.; Ripp, S. L.; Spracklin, D. K.; Tremaine, L. M.; Vaz, A. D. Deuterium isotope effects on drug pharmacokinetics. I. System-dependent effects of specific deuteration with aldehyde oxidase cleared drugs. *Drug Metab. Dispos.* **2012**, *40*, 625−634.

(23) Dahal, U. P.; Joswig-Jones, C.; Jones, J. P. Comparative study of the affinity and metabolism of type I and type II binding quinoline carboxamide analogues by cytochrome P450 3A4. *J. Med. Chem.* **2012**, *55*, 280−290.

(24) Pearson, J.; Dahal, U. P.; Rock, D.; Peng, C. C.; Schenk, J. O.; Joswig-Jones, C.; Jones, J. P. The kinetic mechanism for cytochrome P450 metabolism of Type II binding compounds: Evidence supporting direct reduction. *Arch. Biochem. Biophys.* **2011**, *511*, 69−79.

(25) Chiba, M.; Jin, L.; Neway, W.; Vacca, J. P.; Tata, J. R.; Chapman, K.; Lin, J. H. P450 interaction with HIV protease inhibitors: relationship between metabolic stability, inhibitory potency, and P450 binding spectra. *Drug Metab. Dispos.* **2001**, *29*, 1−3.

(26) Barr, J.; Jones, J. Inhibition of Human Liver Aldehyde Oxidase: Implications for Potential Drug-drug Interactions. *Drug Metab. Dispos.* **2011**, *39*, 2381−2386.

(27) Obach, R. S.; Huynh, P.; Allen, M. C.; Beedham, C. Human liver aldehyde oxidase: inhibition by 239 drugs. *J. Clin. Pharmacol.* **2004**, *44*, 7−19.

(28) Stephans, P. J.; Devlin, F. J.; Chabalowski, C. F.; Frisch, P. J. Ab Initio Calculation of Vibrational Absorption and Circular Dichroism Spectra Using Density Functional Force Fields. *J. Phys. Chem.* **1994**, *98*, 11623−11627.